

## Twin Boundaries Can Be Moved by Step Edges During Film Growth

W. L. Ling, N. C. Bartelt, and K. F. McCarty

*Sandia National Laboratories, Livermore, California 94550, USA*

C. B. Carter

*University of Minnesota, Minneapolis, Minnesota 55455, USA*

(Received 20 May 2005; published 13 October 2005)

We track individual twin boundaries in Ag films on Ru(0001) using low-energy electron microscopy. The twin boundaries, which separate film regions whose close-packed planes are stacked differently, move readily during film growth but relatively little during annealing. The growth-driven motion of twin boundaries occurs as film steps advance across the surface—as a new atomic Ag layer reaches an fcc twin boundary, the advancing step edge carries along the boundary. This coupling of the microstructural defect (twin boundary) and the surface step during growth can produce film regions over 10  $\mu\text{m}$  wide that are twin free.

DOI: [10.1103/PhysRevLett.95.166105](https://doi.org/10.1103/PhysRevLett.95.166105)

PACS numbers: 68.55.Jk, 61.72.Ff, 68.37.Nq, 68.60.Dv

A large body of work exists aimed at understanding the surface roughness that often develops during the growth of thin films [1]. Because the time-dependent positions of surface steps determine the surface roughness, the equations that govern step motion have been discussed in great detail in the literature [2]. However, the technological properties of a film are also determined by features beyond the surface morphology. In particular, the film's grain structure is very important [3]. Such microstructural features, of course, can also evolve with time during growth or annealing. But these processes are often viewed as being independent of surface step motion. Here we show there can be a close connection between morphological evolution and microstructural evolution—we find that the evolution of crystallographic twin boundaries, a common microstructural defect in thin films [3,4], can be determined by surface step motion.

So that defect-free films with ideal behavior can be synthesized, considerable effort has been devoted to minimizing twin boundaries. Twins are generally believed to originate from the nucleation stage of film growth. That is, when film islands nucleate, not all of them contain the same stacking sequence of film layers. Twin boundaries then occur where islands with different stacking sequence impinge [3,5,6]. Attempts to reduce the density of twin boundaries are usually based on minimizing their nucleation (see, for example, [7,8]) or by removing them by annealing [5]. In this Letter we show that twins can be removed during growth even when they are difficult to eliminate by annealing. Furthermore, we use real-time microscopy to identify the process that moves the twin boundaries—they move in conjunction with surface steps advancing during film growth.

The Ag(111) films examined in this study were grown by physical vapor deposition on a step-free region of a Ru(0001) substrate under ultrahigh vacuum conditions in a low-energy electron microscope. Previous work has shown

that Ag grows layer-by-layer in such regions [9]. The atomic-resolution, scanning tunneling microscopy image in Fig. 1 reveals that the 2nd Ag layer is close-packed and has nearly the same in-plane atomic spacing as bulk Ag [10]. Since no dislocations thread through the 2nd layer, it is a defect-free substrate for the growth of subsequent Ag layers. We observe that Ag islands nucleate with two different stacking sequences on the 2nd layer substrate. If we arbitrarily call the stacking of the 2nd layer *A*, the 3rd layer Ag can occupy either *B* sites or *C* sites (i.e., the two nonequivalent three-fold hollow sites). Additional layers follow fcc stacking, i.e., either *ABCA...* or *ACBA...*, as illustrated in Fig. 2(a). Where differently stacked islands impinge, a twin boundary of type  $\Sigma = 3\langle 111 \rangle$  occurs. The atomic structure of these boundaries in fcc metals, which

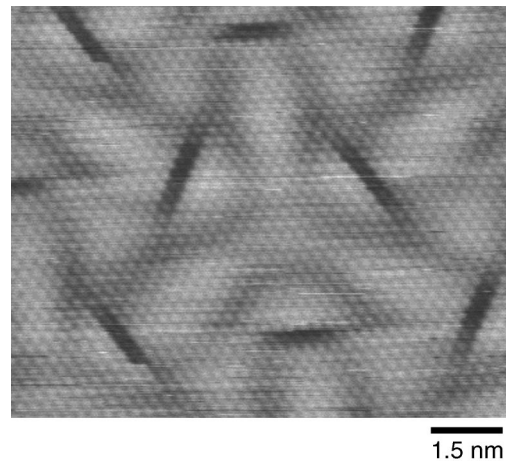


FIG. 1. Scanning tunneling micrograph of 2 ML Ag on Ru(0001) showing a close-packed hexagonal Ag layer. Each bright spot is a Ag atom. The triangular corrugations result from a dislocation network confined to the 1st Ag layer. The dislocations accommodate the large size misfit between the Ag and Ru atoms.

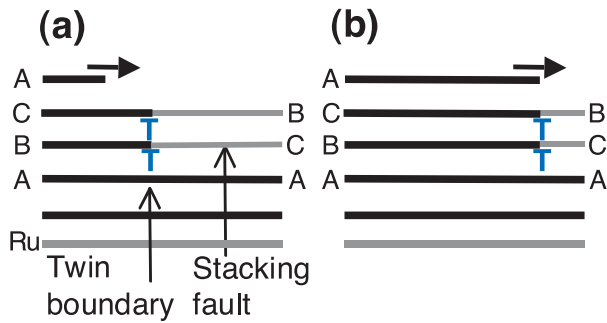


FIG. 2 (color). (a) Schematic illustration of a twin boundary in a Ag(111) film in Ru(0001). A stacking fault in the 3rd Ag layer causes the two film regions next to the boundary to have different stacking sequences. Partial dislocations (blue  $T$  symbols) occur at the twin boundary on each film layer where the stacking changes across the boundary. (b) Illustration of growth-induced twin-boundary motion. The twin boundary moves in lock step with the step edge of the advancing 5th Ag layer; the stacking of the 3rd and 4th layers switches, and the stacking fault shrinks.

typically facet along  $\{112\}$  planes, is well known [11]. Because the stacking changes across the twin boundary, one of the adjacent stacking domains contains a stacking fault [see Fig. 2(a)]. As discussed below, we were unable to remove these twins by annealing—they were essentially static. However, the twin boundaries do not remain static during film growth—they move and reduce the density of stacking faults.

Figure 3(a) shows the spatial distribution of stacking faults present shortly after 3 ML-thick regions have nucleated. In the dark-field low-energy electron microscopy (LEEM) [12] images of Figs. 3(a)–3(d), the two types of 3 ML stacking appear either black or white [13] while 2 ML-thick regions appear gray. The two stacking sequences, arbitrarily labeled as stacking I (black) and II (white), appear with approximate equal abundance. This observation suggests that the two stacking types nucleate essentially randomly on the 2 ML-thick film [14]. When the 3rd layer is complete [Fig. 3(b)], the entire surface is covered by domains of the two stacking types. Well-defined twin boundaries separate the regions of different stacking.

We find that the twin boundaries move as film growth continues. As Figs. 3(b)–3(d) show, the white region of type II stacking shrinks as the film grows. In fact, when the film has thickened to 4.7 ML [Fig. 3(d)], the large domain of type II stacking (white) that ran vertically in Fig. 3(b) has been completely eliminated. That is, the stacking sequence of the type II domain was switched to type I stacking as the film grew.

We next show that stacking domains evolve because their twin boundaries move as they are overgrown by advancing film steps. Figs. 3(e) and 3(f) shows bright-field LEEM images captured at times close to the recording times of Figs. 3(c) and 3(d), respectively. While showing

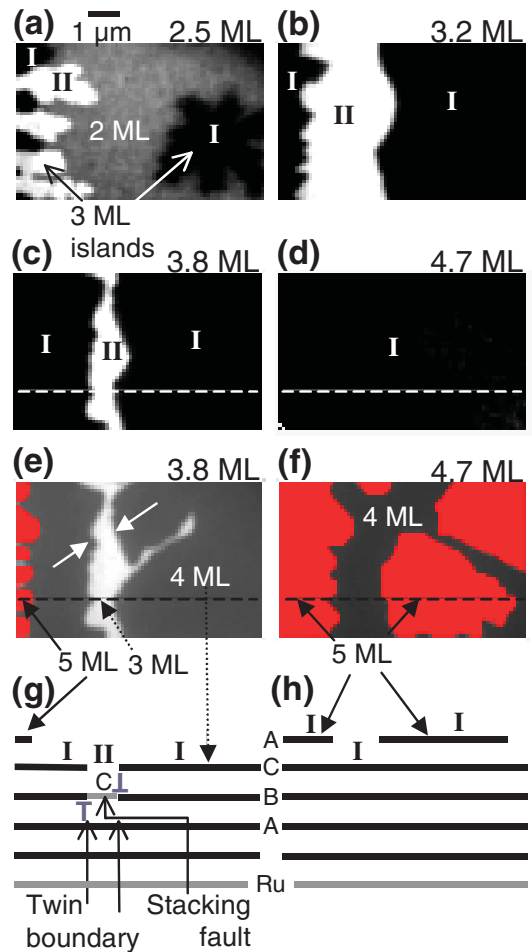


FIG. 3 (color). Twin boundaries being eliminated as Ag steps advance during film growth. (a)–(d) Dark-field LEEM images of (01) diffraction beam showing changes in stacking sequence of 3 ML Ag films during growth at  $180^\circ\text{C}$ . The 3rd Ag layer nucleates randomly in two possible stacking sequences (the black and white domains labeled I and II, respectively) on the 2 ML film (gray) in image (a). By 4.7 ML, image (d), the type II stacking domain has been eliminated. The imaged region contains no substrate steps. (e)–(f) Film-thickness contrast in bright-field images of growing Ag film shown in images (c)–(d). The advancing step edge of the 4th layer (scalloped lines near center marked by white arrows) in image (e) coincides with the twin boundary of image (c). 5 ML-thick regions are colored red. (g)–(h) Schematic cross section of how an advancing film layer causes twin boundaries to move and change the stacking of underlying film layers. Shown are the stacking sequences of the film layers that occur at the location of the dashed horizontal lines shown in images (c)–(f). The dislocations (marked with blue  $T$  symbols) that form the twin boundary move in concert with the 4th Ag layer advancing from the left and right. A domain of type II stacking is eliminated as opposite twinning dislocations annihilate.

no stacking contrast, these images determine the local film thickness [15]. The white region in Fig. 3(c) is 3 ML thick and the adjacent dark regions are 4 ML thick. Furthermore, comparing Figs. 3(c) and 3(e) clearly establishes that the

boundary separating the two stacking types (I and II in Fig. 3(c)) coincides with the surface step that separates the 3 ML and 4 ML regions (the white and gray regions, respectively, in Fig. 3(e)). Obviously, as the step of the 4th layer passes over the type II region, its stacking simultaneously switches to type I.

This boundary-migration mechanism is illustrated schematically in Figs. 3(g) and 3(h): during overgrowth by a Ag layer, the twin boundary moves and switches the stacking in the underlying Ag layer. This mechanism can produce large regions that are free of twin boundaries and stacking faults. In Fig. 3(d), for example, all twins have been removed from a film region over 10  $\mu\text{m}$  wide.

Further confirmation that the twin boundary actually moves comes from the following experiment. During growth, film regions that underwent a stacking change as a Ag step swept over them were identified. Ag was then desorbed layer-by-layer by careful vacuum annealing while imaging to determine the stacking of underlying layers. (As discussed below, such annealing did not cause significant boundary motion.) Notably, we observed that where an overgrown Ag layer had caused a contrast change in the dark-field image, no change occurred when the overlayer was desorbed, establishing that all layers above the second layer irreversibly switched in concert as the Ag layer advanced, as drawn in Fig. 2.

To further understand these observations, Fig. 4 shows atomic (ball) models of four different scenarios of how the film step shown in Fig. 4(a) might propagate as it approaches a twin boundary. In Fig. 4(b), the step has stopped

at the boundary, which separates film regions of different stacking. In Figs. 4(c) and 4(d), the step has overgrown the twin boundary, which has not moved. In Fig. 4(e), however, the step has advanced and carried the boundary with it, as observed experimentally (Figs. 2 and 3). We next discuss when each scenario might occur and why scenario 4(e) occurs in our system.

If the film step stopped moving when it reached the twin boundary [Fig. 4(b)], the initially formed domain structure would propagate through the thickening film, as is often assumed. (Even if a layer cannot be completed because a step does not advance past a twin boundary, the layer would fill in by new islands nucleating elsewhere and expanding.) Stopping the step would either require that the energy barrier for adatom attachment be large when the step edge lies over the twin boundary [Fig. 4(b)] (so that adatoms never attach to the step edge), or that the Ag adatom mobility be very high (so that any adatom attaching at a step edge on a boundary quickly detaches and diffuses to a lower energy step elsewhere). Two ways that the Ag layer can advance without changing the stacking of the underlying Ag layer are shown in Figs. 4(c) and 4(d). The available binding sites are not optimal—Figs. 4(c) and 4(d) show that the atoms will be incorporated by binding at bridge sites at the boundary or by creating regions of hcp stacking, respectively. However, the energies of bridge sites and stacking faults are probably small compared to the binding energy of adatoms to step edges. While these processes [Figs. 4(c) and 4(d)] seem plausible, they did not occur in our system, however, as shown by the lack of

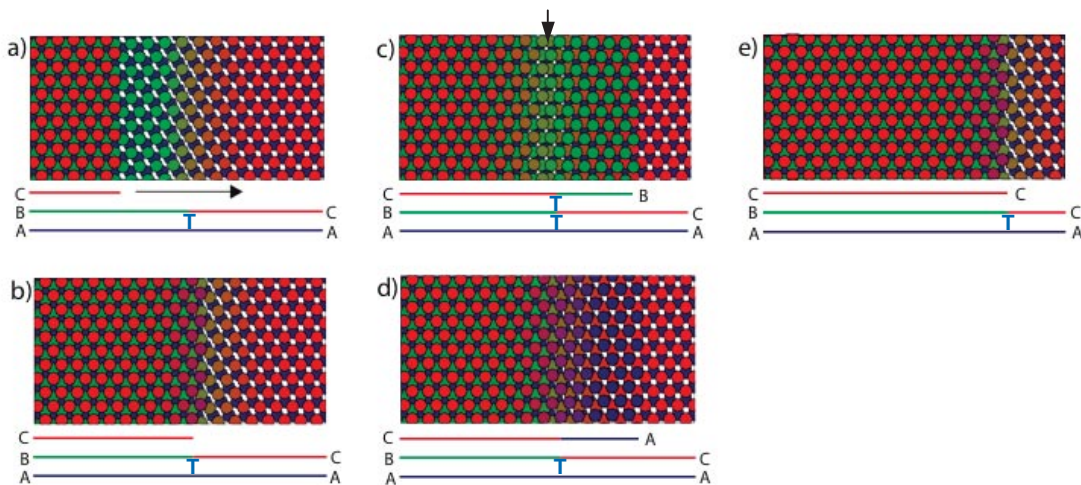


FIG. 4 (color). Possible atomic arrangements that could result from a Ag layer overgrowing a stacking fault. The circles represent three layers of Ag atoms color coded by their stacking arrangement. The horizontal lines show the Ag layers in cross section, also color coded and labeled by their stacking type. In (a) a step advances from the left towards a twin boundary that bounds a stacking fault. The Shockley partial dislocation (the upright and inverted  $T$  symbols) at the twin boundary changes the stacking of the 2nd Ag layer from  $B$  to  $C$ . In (b), the step of the 3rd layer has stopped at the twin boundary. In (c)–(e), the step has advanced further, but with three different scenarios of the Ag-layer stacking. In (c) and (d), the original twin boundary does not move. In (c) fcc stacking is maintained on either side of the boundary but the top Ag layer contains atoms in unfavorable twofold bridge sites (vertical arrow) at the twin boundary. (The twin boundary thickens by one layer and the stacking fault in the 2nd layer does not shrink.) In (d) all atoms are in energetically favorable threefold hollow sites but unfavorable hcp ( $ACA$ ) stacking occurs. Scenario (e) matches experiment—the twin boundary moves in concert with the advancing film step and the stacking fault in the 2nd film layer shrinks.



contrast in Fig. 3(d) and the desorption experiment described above. Instead, as shown in Fig. 4(e), the domain boundary was carried along with the film step edge. Thus, the twin-boundary–migration process must have a relatively low-energy barrier. It is reasonable for this barrier to be small because the partial dislocations [the “T” symbols in Figs. 2, 3(g), and 4] that comprise the twin boundary move by glide [5], a process with a small energy barrier [16,17]. Thus, the boundary motion we observe depends on a low barrier for dislocation glide in the Ag film layers.

We have also observed twin boundaries moving (and switching the stacking of Ag layers) as 5th-layer Ag steps advance over a stacking fault (see Fig. 2). In this case, two dislocations [those at the 3rd and 4th Ag layers in Fig. 2(a)] move by glide when the boundary advances. Moving the twin boundary should become increasingly difficult as the Ag film thickens because each additional Ag layer contains a dislocation. Thus, boundary migration becomes less common as the film gets thicker. Therefore, the mechanism we observe can eliminate stacking faults and reduce twin-boundary length, but only in the initial stages of film growth.

Unlike during growth at relatively low temperature (180 °C), significant twin-boundary motion did not occur during annealing in the absence of a Ag flux, even at temperatures high enough to cause film desorption (~450 °C). Our observation that boundaries move readily during growth but little during annealing might at first seem surprising because twin boundaries cost energy and the system’s energy is lowered by eliminating them. Decreasing the system’s free energy by eliminating the boundaries provides a driving force (the Gibbs-Thomson force, which is proportional to the local boundary curvature) to move the boundary. However, our observations show that this driving force alone is not sufficient to move the twin boundaries at appreciable rates, even at elevated temperature. The incorporation of adatoms into steps during growth provides an additional driving force that is large enough to move the partial dislocations, and, thus, the twin boundaries.

We note that the stacking faults that form during the homoepitaxial growth of Ir seem to evolve by a distinctly different atomic mechanism [18]. This difference could be due to the fact that at least some of the stacking-fault (twin) boundaries in Ir consist of distinct high-energy lines of vacancies rather than the broader low-energy partial dislocations characteristic of the boundaries in Ag and Cu [19] films on Ru. Apparently, the sharp Ir vacancy lines cannot easily glide, as required for the mechanism we propose here.

In summary, this work shows that a film’s morphology and its microstructure can be intimately coupled. That is, we find an unanticipated process in which the twin boundaries that separate stacking-fault domains move in lock step

with the step edges of advancing film layers. Because of this coupling of surface step motion to microstructural evolution, the stacking faults that form in the initial stages of film growth do not necessarily remain static. Thus, despite initially nucleating many stacking faults, we observe large twin-free film regions after film steps have advanced across the surface during growth.

This work was supported by the Office of Basic Energy Sciences, Division of Materials Sciences of the U.S. DOE under Contract No. DE-AC04-94AL85000. The authors thank D. L. Medlin for helpful discussions.

- 
- [1] A. Pimpinelli and J. Villain, *Physics of Crystal Growth* (Cambridge University Press, New York, 1998).
  - [2] H. C. Jeong and E. D. Williams, *Surf. Sci. Rep.* **34**, 171 (1999).
  - [3] M. Ohring, *The Materials Science of Thin Films* (Academic Press, San Diego, 2002), 2nd ed..
  - [4] G. P. Dimitrakopoulos, P. Komninou, and R. C. Pond, *Phys. Status Solidi B* **227**, 45 (2001).
  - [5] M. J. Stowell, in *Epitaxial Growth, Part B*, edited by J. W. Matthews (Academic Press, New York, 1975), p. 437.
  - [6] A. H. King, *Phys. Status Solidi A* **76**, 629 (1983).
  - [7] J. Camarero, T. Graf, J. J. de Miguel, R. Miranda, W. Kuch, M. Zharnikov, A. Dittschar, C. M. Schneider, and J. Kirschner, *Phys. Rev. Lett.* **76**, 4428 (1996).
  - [8] Y. Garreau, A. Coati, A. Zobelli, and J. Creuze, *Phys. Rev. Lett.* **91**, 116101 (2003).
  - [9] W. L. Ling, T. Giessel, K. Thurmer, R. Q. Hwang, N. C. Bartelt, and K. F. McCarty, *Surf. Sci.* **570**, L297 (2004).
  - [10] W. L. Ling, J. de la Figuera, N. C. Bartelt, R. Q. Hwang, A. K. Schmid, G. E. Thayer, and J. C. Hamilton, *Phys. Rev. Lett.* **92**, 116102 (2004).
  - [11] R. C. Pond and V. Vitek, *Proc. R. Soc. A* **357**, 453 (1977).
  - [12] E. Bauer, *Rep. Prog. Phys.* **57**, 895 (1994).
  - [13] The AB and AC stackings each produce a hexagonal array of low-energy electron diffraction spots in which weak and strong spots alternate to give three-fold symmetry. The relative intensities of the first-order diffraction spots reverse between the two stacking types. Therefore, in a dark-field image formed from a first-order diffraction spot, one stacking type appears dark and the other bright.
  - [14] K. Meinel, M. Klaua, and H. Bethge, *Phys. Status Solidi A* **110**, 189 (1988).
  - [15] M. S. Altman, W. F. Chung, and C. H. Liu, *Surf. Rev. Lett.* **5**, 1129 (1998).
  - [16] J. P. Hirth and J. Lothe, *Theory of Dislocations* (John Wiley, New York, 1982), p. 240.
  - [17] Glide at the Ag/Ru interface enabled by the dislocation structure in the first Ag layer may also contribute to boundary migration (See Ref. [10]).
  - [18] C. Busse and T. Michely, *Surf. Sci.* **552**, 281 (2004).
  - [19] F. El Gabaly, W. L. Ling, K. F. McCarty, and J. de la Figuera, *Science* **308**, 1303 (2005).